J. Fluid Mech. (2006), *vol.* 553, *pp.* 401–418. © 2006 Cambridge University Press
doi:10.1017/S0022112006009165 Printed in the United Kingdom

Dynamo action in a rotating convective layer

By FAUSTO CATTANEO[1] AND DAVID W. HUGHES[2]

[1]Department of Astronomy and Astrophysics, University of Chicago, Chicago, IL 60637, USA
[2]Department of Applied Mathematics, University of Leeds, Leeds LS2 9JT, UK

(Received 17 February 2005 and in revised form 10 October 2005)

We study dynamo processes in a convective layer of Boussinesq fluid rotating about the vertical. Irrespective of rotation, if the magnetic Reynolds number is large enough, the convection acts as an efficient small-scale dynamo with a growth time comparable with the turnover time and capable of generating a substantial amount of magnetic energy. When the rotation is important (large Taylor number) the characteristic horizontal scale of the convection decreases and the flow develops a well-defined distribution of kinetic helicity antisymmetric about the mid-plane. We find no convincing evidence of large-scale dynamo action associated with this helicity distribution. Even when the rotation is strong, the magnetic energy at large scales remains small, and comparable with that in the non-rotating case. By externally imposing a uniform field, we measure the average electromotive force. We find this quantity to be extremely strongly fluctuating, and are able to compute the associated α-effect only after very long time averaging. In those cases for which reasonable convergence is achieved, the α-effect is small, and controlled by the magnetic diffusivity. Thus we demonstrate the existence of a system whose small-scale dynamo growth rate is turbulent, i.e. independent of diffusivity, but whose α-effect is laminar, i.e. dependent on diffusivity. The implications of these results to the problem of the generation of strong mean fields are discussed.

1. Introduction

Dynamo action is commonly invoked to explain the origin of magnetic fields in the universe. In a hydromagnetic dynamo, kinetic energy is converted into magnetic energy throughout the bulk of an electrically conducting fluid, thereby maintaining some level of magnetization for times longer than the Ohmic decay time. For mathematical reasons it is often convenient to distinguish between the process of field amplification from an initial state of weak magnetization – the kinematic problem – and the process of growth saturation and field maintenance – the dynamic problem. The former is linear, requiring the solution of the induction equation for prescribed velocities; the latter is nonlinear, involving the simultaneous solution of the induction and momentum equations. It is also helpful to make the distinction between small-scale dynamos, in which the magnetic field exists on a scale comparable with or smaller than those of the driving flow, and large-scale dynamos, which possess significant energy on scales much larger than those of the velocity field.

A major revolution took place in dynamo theory during the 1950s and 1960s with the development and formalization of mean field electrodynamics (Parker 1955; Braginskii 1964; Steenbeck, Krause & Rädler 1966). A crucial feature of this theory is that it shifts the emphasis from the magnetic field itself to the average magnetic

https://doi.org/10.1017/S0022112006009165 Published online by Cambridge University Press

field. Whereas the former can display strong fluctuations, the latter is assumed to be smoother, and therefore, in some sense, more mathematically tractable. The resulting theory has dominated the modelling of astrophysical dynamos since that time. In mean field theory, the effects of fluctuations on the mean field evolution are represented by a number of transport coefficients. These are tensor quantities which, under suitable circumstances, have straightforward physical interpretations in terms of average induction (the celebrated α-effect), average turbulent diffusion (the β-effect), average advection (the γ-effect) and so on. Models of astrophysical dynamos are often discussed in terms of the properties of these coefficients, such as their spatial variations, symmetries, relative magnitudes, etc. Indeed, the specification of these coefficients essentially defines a mean field dynamo model. Whereas β and γ represent turbulent enhancements of diffusion and advection, physical effects that are present in the induction equation before averaging, the coefficient α introduces a remarkable new effect that is at the heart of the success of mean field dynamo theory. One of the most important results of mean field electrodynamics is to establish a relationship between α and the lack of reflectional symmetry of the underlying turbulence.

Two significant difficulties arise when attempting to use mean field theory to model astrophysical magnetic fields. One is that mean field theory is intrinsically kinematic; the other is that of determining the transport coefficients from a knowledge of the statistical properties of the fluctuations – even in the kinematic regime. In order to be specific about the nature of the problems, we write out the basic building blocks of mean field theory. The mean induction equation is given by

$$(\partial_t - \eta\nabla^2)\langle \boldsymbol{B}\rangle = \nabla \times \boldsymbol{\mathscr{E}}, \tag{1.1}$$

where $\langle \boldsymbol{B}\rangle$ is some suitable average of the magnetic field, η is the collisional diffusivity, and the mean emf $\boldsymbol{\mathscr{E}} = \langle \boldsymbol{u} \times \boldsymbol{b}\rangle$, where we have assumed that the velocity $\boldsymbol{u}$ has no mean. The fluctuating component of the magnetic field $\boldsymbol{b}$ satisfies the equation

$$(\partial_t - \eta\nabla^2)\boldsymbol{b} = \nabla \times (\boldsymbol{u} \times \langle \boldsymbol{B}\rangle) + \nabla \times \boldsymbol{G}, \tag{1.2}$$

where $\boldsymbol{G} = \boldsymbol{u} \times \boldsymbol{b} - \langle \boldsymbol{u} \times \boldsymbol{b}\rangle$. The linearity of (1.2) in $\boldsymbol{b}$ establishes a linear relation between $\boldsymbol{\mathscr{E}}$ and $\langle \boldsymbol{B}\rangle$ of the form

$$\mathscr{E}_i = \alpha_{ij}\langle \boldsymbol{B}\rangle_j + \beta_{ijk}\partial_j\langle \boldsymbol{B}\rangle_k + \ldots, \tag{1.3}$$

which formally closes the system. In the kinematic regime, the coefficients α_{ij}, β_{ijk}, etc. do not depend on $\langle \boldsymbol{B}\rangle$ and are determined solely by η and the statistical properties of $\boldsymbol{u}$.

If the term in $\boldsymbol{G}$ can be neglected in (1.2) (the so-called first-order smoothing approximation) it is then possible to solve for $\boldsymbol{b}$ in terms of $\boldsymbol{u}$ and $\langle \boldsymbol{B}\rangle$, and hence to obtain explicit expressions for the transport coefficients. There are two limits in which this can be achieved. One is when the correlation time τ of the turbulence is short compared with the turnover time, in which case α is given by

$$\alpha = -\tfrac{1}{3}\tau\langle \boldsymbol{u}\cdot\boldsymbol{\omega}\rangle, \tag{1.4}$$

where $\boldsymbol{\omega}$ is the vorticity, and we have assumed $\alpha_{ij} = \alpha\delta_{ij}$ (isotropy) (see, for example, Krause & Rädler 1980). The important thing about this expression is that it contains the flow helicity, and therefore makes explicit the relationship between the α-effect and the lack of reflectional symmetry of the flow. The other tractable limit is that of large η (small magnetic Reynolds number Rm), in which case another closed form expression for α can be obtained which also involves the helicity (see Moffatt 1978). For these cases, the determination of the transport coefficients has predictive power;

https://doi.org/10.1017/S0022112006009165 Published online by Cambridge University Press

they can be used in equation (1.1) explicitly to determine the evolution of the mean field (at least in the kinematic regime). In all other cases it is impossible to obtain a closed form, analytic expression for $\boldsymbol{b}$ in terms of $\boldsymbol{u}$; equation (1.2) must be solved somehow (typically numerically) in order for the coefficients to be computed. Here, we might regard knowledge of these coefficients as having interpretative value.

At the heart of the formulation outlined above is the assumption that $\boldsymbol{u}$ is prescribed, and hence statistically independent of $\boldsymbol{B}$. This clearly cannot be the case in the nonlinear regime, when the Lorentz force affects the form of $\boldsymbol{u}$. If we wish to describe the nonlinear evolution of the mean magnetic field within the framework of mean field theory, then it is necessary to confront the problem of closure. There are two generic approaches. Following from the early work of Jepps (1975) and Yoshimura (1975), one approach is to use phenomenological arguments to obtain expressions for the transport coefficients that are physically plausible. The problem with this approach is that there is disagreement over which phenomenology should be incorporated. For example, there is considerable controversy over the strength of the mean field needed to cause a significant reduction of the turbulent α-effect from its kinematic value (Vainshtein & Cattaneo 1992; Kulsrud & Anderson 1992; Gruzinov & Diamond 1994; Cattaneo & Hughes 1996; Field, Blackman & Chou 1999; Blackman & Field 2000). The other is to treat the induction and momentum equations on an equal footing, and to use the standard machinery of closure theory to obtain tractable equations (e.g. Pouquet, Frisch & Léorat 1976; Rüdiger 1989). The problem here is that greater mathematical complexity does not necessarily guarantee a better result.

Most astrophysical situations involve flows with large magnetic Reynolds numbers, correlation times of order unity, and strong nonlinear behaviour. Nonetheless, mean field theory is often used in astrophysical modelling, on the assumption that expressions of the type (1.4), suitably modified to allow for nonlinear effects, can still be used to provide estimates of the transport coefficients. The validity of this assumption nevertheless remains to be verified. Given the complexity of the problem, its verification is unlikely to come from rigorous mathematics in the immediate future. Current laboratory experiments are limited to moderate values of the magnetic Reynolds number, even though there has been remarkable progress in recent times. Another possibility is to turn to numerical experiments that can reach moderately high values of Rm (though nowhere near the values that pertain astrophysically) to guide our physical intuition. Our aim in this paper is to consider the astrophysically motivated problem of dynamo action in a rotating layer of convecting fluid. This is a very natural system to study, and has been considered previously by Childress & Soward (1972), Soward (1974), St Pierre (1993), Jones & Roberts (2000), Rotvig & Jones (2002) and Stellmach & Hansen (2004). Turbulent convection, even in the absence of rotation, acts as a small-scale dynamo (Meneguzzi & Pouquet 1989; Cattaneo 1999); rotation then introduces a lack of reflectional symmetry and hence the possibility of an α-effect. Furthermore, this system can be treated with great computational efficiency, so that we can consider moderately high magnetic Reynolds numbers in a system of sufficient horizontal extent to accommodate many convective cells.

2. Formulation

We consider thermally driven convection in a three-dimensional Cartesian layer of incompressible (Boussinesq) fluid rotating about the vertical. The fluid layer has depth d, angular velocity Ω, density ρ, kinematic viscosity ν, thermal diffusivity κ

https://doi.org/10.1017/S0022112006009165 Published online by Cambridge University Press

and magnetic diffusivity η. Following standard practice, we adopt the layer depth d, the thermal relaxation time d^2/κ, and the temperature drop across the layer ΔT as the units of length, time and temperature, respectively. We measure magnetic field intensities in units of the equivalent Alfvén speed $B/\sqrt{\mu_0\rho}$, where μ_0 is the magnetic permeability of the medium. With these units, and in standard notation, the evolution equations read

$$(\partial_t - \sigma\nabla^2)\boldsymbol{u} + \boldsymbol{u}\cdot\nabla\boldsymbol{u} + \sigma Ta^{1/2}\boldsymbol{e}_z \times \boldsymbol{u} = -\nabla p + \boldsymbol{J}\times\boldsymbol{B} + \sigma Ra\,\theta\boldsymbol{e}_z, \tag{2.1}$$

$$(\partial_t - \sigma/\sigma_m\nabla^2)\boldsymbol{B} + \boldsymbol{u}\cdot\nabla\boldsymbol{B} = \boldsymbol{B}\cdot\nabla\boldsymbol{u}, \tag{2.2}$$

$$(\partial_t - \nabla^2)\,\theta + \boldsymbol{u}\cdot\nabla\theta = w, \tag{2.3}$$

$$\nabla\cdot\boldsymbol{B} = \nabla\cdot\boldsymbol{u} = 0, \tag{2.4}$$

where $\boldsymbol{J} = \nabla\times\boldsymbol{B}$ is the current density, w is the vertical velocity, and θ denotes the temperature fluctuations relative to a linear background profile (e.g. Chandrasekhar 1961). Four dimensionless numbers appear explicitly: the Rayleigh number $Ra = g\tilde{\alpha}\tilde{\beta}d^4/\kappa\nu$ (where g is the accleration due to gravity, $\tilde{\alpha}$ is the coefficient of thermal expansion and $\tilde{\beta}$ is the superadiabatic temperature gradient), which measures the strength of thermal buoyancy relative to dissipation; the Taylor number $Ta = 4\Omega^2 d^4/\nu^2$, and the kinetic and magnetic Prandtl numbers

$$\sigma = \frac{\nu}{\kappa}, \quad \sigma_m = \frac{\nu}{\eta}. \tag{2.5}$$

In the horizontal directions, we assume that all fields are periodic with periodicity λ. In the vertical, we consider standard illustrative boundary conditions on the temperature and velocity fields, namely that the boundaries are perfect thermal conductors, impermeable and stress-free. Formally these correspond to

$$\theta = w = \partial_z u = \partial_z v = 0 \quad \text{at } z = 0, 1. \tag{2.6}$$

There are two obvious possibilities for the choice of magnetic boundary condition, namely that the boundaries are either perfectly conducting or are insulating. One of the purposes of this work is to consider the evolution of mean quantities, which involves a definition of averages. The natural average in this system is one over horizontal planes, which involves averaging over many convective cells. From the point of view of generating large-scale fields with the simplest vertical structure, it is therefore preferable to choose perfectly conducting boundary conditions, for which the field is purely horizontal, thereby admitting field configurations with only one node in the vertical. Thus, we choose

$$B_z = \partial_z B_x = \partial_z B_y = 0 \quad \text{at } z = 0, 1. \tag{2.7}$$

In this system, the importance of rotation is controlled by both the Taylor and Rayleigh numbers. We want to explore regimes in which the convection is vigorous and rotation is significant, so that the resulting flows are helical. These requirements dictate that Ra and Ta are comparable and $\gtrsim 10^5$. Substantially larger values become computationally difficult; as a compromise, we choose to fix $Ta = 5\times10^5$ and vary Ra accordingly. In what follows we also fix σ to be unity. In order to limit the effects of the boundaries in the horizontal it is important to have reasonably large values of λ; the computations described herein were all carried out with $\lambda = 5$ or $\lambda = 10$.

We solve equations (2.1)–(2.4) numerically by standard pseudospectral methods optimized for machines with parallel architecture. Details concerning the numerical methods can be found in Cattaneo, Emonet & Weiss (2003). The numerical resolution

https://doi.org/10.1017/S0022112006009165 Published online by Cambridge University Press

Ra	Ta	σ	σ_m	λ	B_0	$N_x \times N_y \times N_z$
5×10^5	0	1	5.0	10	0	$512 \times 512 \times 97$
10^6	5×10^5	1	5.0	10	0	$512 \times 512 \times 97$
10^6	5×10^5	1	5.0	5	10	$256 \times 256 \times 97$
6.2×10^4	5×10^5	1	5.0	5	0	$128 \times 128 \times 65$
7×10^4	5×10^5	1	5.0	5	0	$128 \times 128 \times 65$
1.5×10^5	5×10^5	1	5.0	5	0	$256 \times 256 \times 97$
5×10^5	5×10^5	1	5.0	5	0	$256 \times 256 \times 97$
5×10^5	5×10^5	1	5.0	5	1	$256 \times 256 \times 97$
5×10^5	5×10^5	1	5.0	5	10	$256 \times 256 \times 97$
5×10^5	5×10^5	1	5.0	5	100	$256 \times 256 \times 97$
1.5×10^5	5×10^5	1	5.0	5	1	$256 \times 256 \times 97$
1.5×10^5	5×10^5	1	2.5	5	1	$256 \times 256 \times 97$
1.5×10^5	5×10^5	1	1.0	5	1	$256 \times 256 \times 97$

TABLE 1. Summary of the numerical resolution and parameter values for the simulations.

and parameter values for all the simulations presented in this paper are summarized in table 1.

3. Hydrodynamical considerations

In this section we discuss the pertinent features of purely hydrodynamic rotating convection in the absence of magnetic field. For Prandtl numbers greater than or equal to unity, convection sets in as a direct instability, the critical Rayleigh number being given by

$$Ra_c = Ra_0 + \frac{\pi^2 Ta}{k_h^2}, \tag{3.1}$$

where $k_h^2 = k_x^2 + k_y^2$, and $Ra_0 = (\pi^2 + k_h^2)^3/k_h^2$ is the critical value for convection in the absence of rotation (Chandrasekhar 1961). We should note that for large values of Ta, the horizontal wavenumber that minimizes (3.1) behaves like $k_h \sim Ta^{1/6}$, so that for strong rotation, convection sets in as narrow cells. For our choice of Taylor number ($Ta = 5 \times 10^5$), Ra_c takes its minimum value of $Ra_c = 59\,008$ with $k_h = 11.4$.

For extended systems with $\lambda = 5$, say, steady convection exists only in a very narrow parameter range near onset; in general, the convection is time-dependent. As the Rayleigh number increases, the convection changes from a disordered pattern of undulating rolls to a disordered pattern of time-dependent cells whose characteristic horizontal size increases slowly with Ra. These properties are illustrated in figure 1, which shows the temperature distribution in a horizontal plane near the upper boundary for four different values of Ra. When the convection is mostly in the form of rolls, the Coriolis force is such as to drive a flow along the rolls, but with opposite directions in the upper and lower half-planes. The resulting helicity distribution is readily calculated to be positive in the lower half-plane ($z < 0.5$) and negative in the upper half-plane. For higher values of Ra, for which the motion is cellular, the horizontal flows near the upper boundary converge to the downflowing cellular corners; the effect of the Coriolis force is then to impart a net anti-clockwise circulation (viewed from above), which gives rise to a negative correlation between vertical vorticity and vertical velocity. A similar correlation is achieved by the expanding upflows in cellular interiors. At the lower boundary, the effects are reversed and

https://doi.org/10.1017/S0022112006009165 Published online by Cambridge University Press

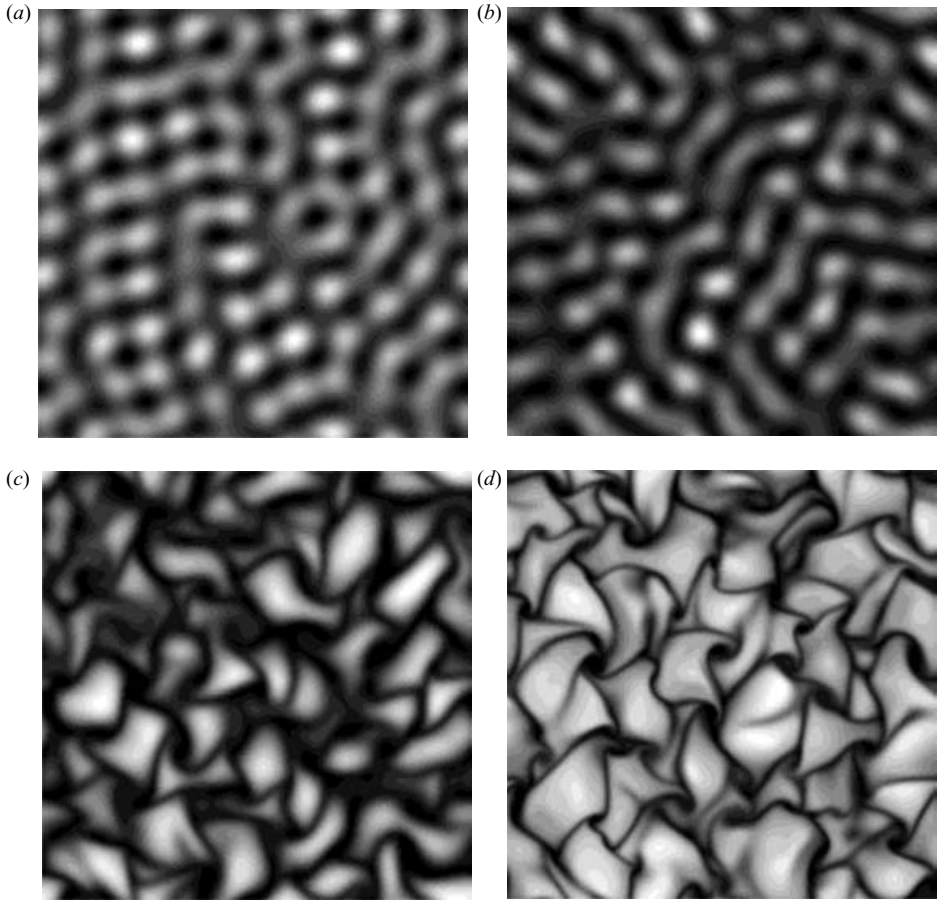


FIGURE 1. Density plots of temperature fluctuations near the upper surface ($z = 0.95$). Light (dark) tones correspond to hot (cold) fluid. All cases have $\lambda = 5$, $Ta = 5 \times 10^5$; (*a*) $Ra = 6.2 \times 10^4$, (*b*) $Ra = 7 \times 10^4$, (*c*) $Ra = 1.5 \times 10^5$ and (*d*) $Ra = 5 \times 10^5$. The transition from convective rolls to disordered cells is apparent.

there exists a positive correlation between velocity and vorticity. Consequently, the net effect of the Coriolis force, for both roll-type and cellular convection, is to ensure that the contributions to the total helicity are of opposite signs in the upper and lower regions. For Boussinesq convection, for which there is an up-down symmetry, the time-averaged helicity distribution is exactly antisymmetric about the mid-plane. At each depth, we define the relative helicity by

$$h(z) = \frac{\langle \boldsymbol{u} \cdot \nabla \times \boldsymbol{u} \rangle}{\langle \boldsymbol{u}^2 \rangle^{1/2} \langle (\nabla \times \boldsymbol{u})^2 \rangle^{1/2}}, \tag{3.2}$$

where the averages are over horizontal planes. Figure 2 shows the instantaneous distribution of $h(z)$ for the cases corresponding to figure 1. When the convection is in the form of rolls ($Ra = 70\,000$), the relative helicity is sinusoidal and almost attains its extreme values (± 1). As Ra is increased, the locations of the extrema of $h(z)$ move towards the boundaries and their magnitudes decrease. For this system with fixed Taylor number, increasing the Rayleigh number increases the vigour of the convection, with the kinetic energy scaling roughly as Ra, and decreases the influence

https://doi.org/10.1017/S0022112006009165 Published online by Cambridge University Press

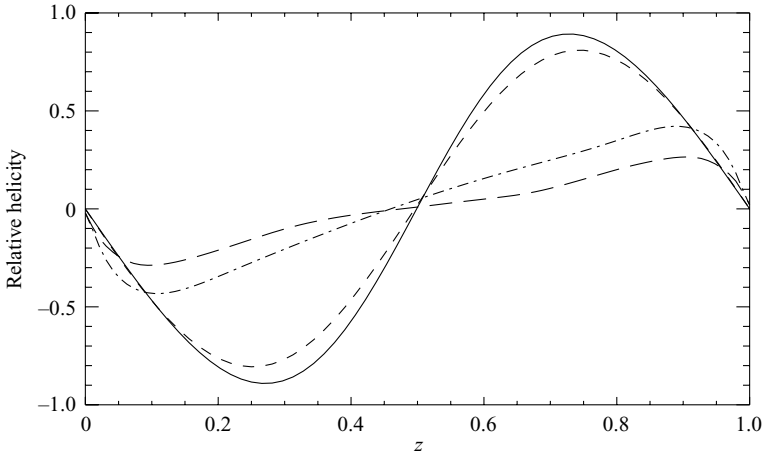


FIGURE 2. Snapshots of $h(z)$ (the horizontally averaged relative flow helicity) for the four cases shown in figure 1: $\lambda = 5$, $Ta = 5 \times 10^5$, and $Ra = 6.2 \times 10^4$, $Ra = 7 \times 10^4$, $Ra = 1.5 \times 10^5$, and $Ra = 5 \times 10^5$. The helicity decreases with increasing Ra. Exact antisymmetry about the mid-plane ($z = 0.5$) is recovered by time averaging.

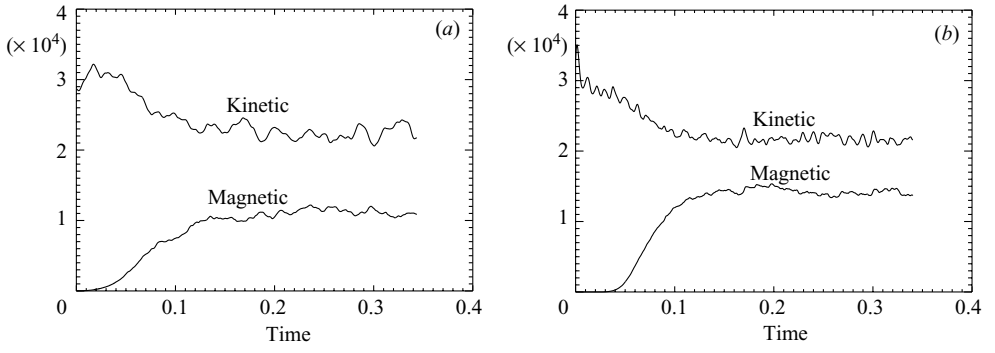


FIGURE 3. Time histories of the kinetic and magnetic energy densities for two cases with $\lambda = 10$, and (*a*) $Ta = 0$, $Ra = 5 \times 10^5$, and (*b*) $Ta = 5 \times 10^5$, $Ra = 10^6$. The magnetic energy density has been multiplied by 3.

of the rotation, with a corresponding slight increase in cell size. It should nevertheless be noted that even in the case with $Ra = 10^6$ – the highest value considered in this paper – the flow is still substantially helical.

4. A representative case

We wish to investigate dynamo action in a case in which rotation is important, convection is vigorous, and the horizontal extent of the domain is large enough that horizontal averages encompass many convective cells. We do this by choosing $Ta = 5 \times 10^5$, $Ra = 10^6$ and $\lambda = 10$. Also, for comparison, we consider a non-rotating case ($Ta = 0$) with the same value of λ and with $Ra = 5 \times 10^5$, chosen such that the magnetic Reynolds numbers for the two cases are approximately the same. Both cases display healthy dynamo properties, as illustrated in figure 3, which shows the time evolution of the kinetic and magnetic energy densities. Initially, the magnetic energy grows exponentially, eventually to reach a stationary state; during this phase the

https://doi.org/10.1017/S0022112006009165 Published online by Cambridge University Press

kinetic energy has a corresponding slight decrease. In the kinematic phase the r.m.s. velocity is approximately 250 for both cases, decreasing to approximately 200 in the nonlinear regime. These values can be used to define kinetic and magnetic Reynolds numbers by

$$Re = \frac{u_{rms}}{\sigma}, \quad Rm = \frac{u_{rms}\sigma_m}{\sigma}; \tag{4.1}$$

also, their inverses give useful estimates of the turnover times. It is important to note that the growth times for both cases are comparable with the turnover times. More specifically, the growth time for the rotating case is $1/78$ (i.e. roughly three turnover times), approximately 400 times shorter than the Ohmic diffusion time. It is therefore reasonable to conclude that both dynamos operate on the turbulent (fast) time scale. In the nonlinear regime, the saturation levels for the magnetic energies are 16% and 22% of the kinetic energies for the non-rotating and rotating cases, respectively.

Some of the morphological differences between the two cases can be seen in figure 4, which shows density plots of the temperature fluctuations, vertical vorticity and x-component of the magnetic field. The most striking feature is the reduction in cell size owing to rotation, which is also reflected in the finer structure of the magnetic fluctuations. Since the stronger fields tend to concentrate in the cellular corners, this property naturally accounts for the slightly higher level of magnetic energy in the rotating case, i.e. the peak fields are comparable in both cases, but with rotation there are more cellular corners per unit area. The vertical vorticity is also concentrated at the cellular corners; but, whereas without rotation vorticity of either sign is equally likely, with rotation one sign becomes dominant.

The preceding considerations show a remarkable similarity between the dynamos in the rotating and non-rotating cases: similar growth rates and similar saturation levels. However, the expectation from mean field theory is that the lack of reflectional symmetry introduced by rotation should lead to some fundamental differences between the two cases. Specifically, the helical nature of the rotating flows should induce an α-effect, leading to the growth of magnetic field on large scales. In the present case, the simplest large-scale field compatible with the boundary conditions and the antisymmetric distribution of flow helicity about the mid-plane is a horizontal field dependent only on z and itself antisymmetric about the mid-plane. Such a field, if present with substantial amplitude, should be detectable by horizontal averaging. Figure 5(a) shows the horizontally averaged kinetic and magnetic energies as a function of z for both cases. The distributions of energy for the two cases are very similar, with a nearly constant value in the interior and a slight increase near the boundaries, most probably associated with the horizontal flows. In figure 5(b), we plot the quantity

$$\Gamma(z) = \frac{|\langle \boldsymbol{B} \rangle|^2}{\langle |\boldsymbol{B}|^2 \rangle}, \tag{4.2}$$

where the angle brackets denote horizontal averages. It can be seen that Γ is a measure of the strength of the large-scale field relative to the total strength. From symmetry considerations, we expect this quantity to be small in the non-rotating case. Remarkably, in view of the general expectations from mean field arguments, it appears to be equally small even in the rotating case. The fact that the profiles are not symmetric about $z = 1/2$, even after some time-averaging, is a reflection of their pitifully small magnitudes (cf. the profiles in figure 5a). This result is also reflected in the horizontal power spectra in figure 6, confirming that the power in the low wavenumber part of the spectrum is tiny compared with the total power. The

https://doi.org/10.1017/S0022112006009165 Published online by Cambridge University Press

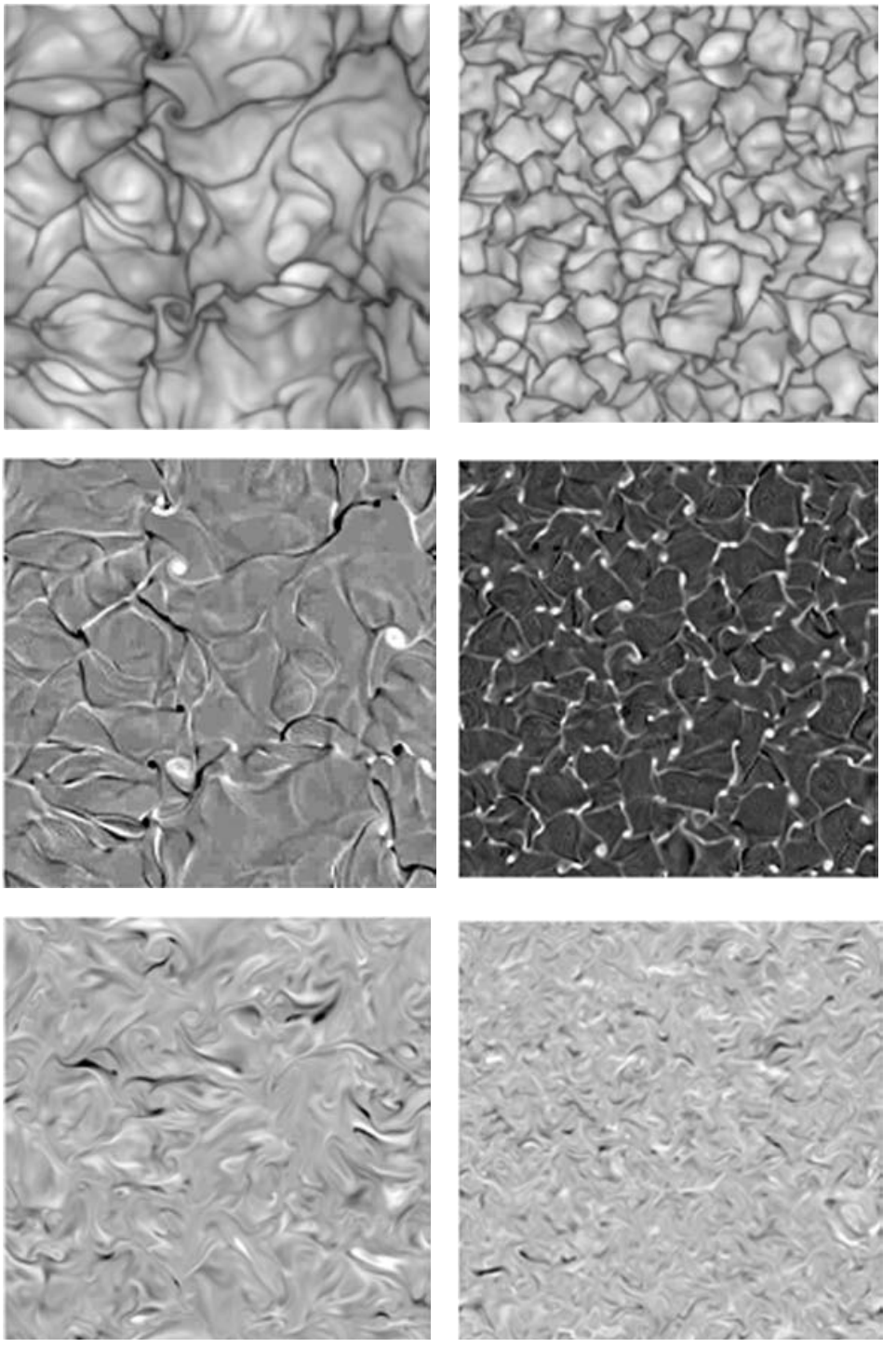


FIGURE 4. Density plots of temperature fluctuations, z-component of the vorticity, and x-component of the magnetic field near the upper boundary ($z = 0.98$) for cases with and without rotation. Light (dark) tones represent positive (negative) fluctuations. The left-hand column corresponds to the non-rotating case with $Ta = 0$, $Ra = 5 \times 10^5$, the right-hand column to the case with rotation, $Ta = 5 \times 10^5$, $Ra = 10^6$. In both cases $\lambda = 10$.

https://doi.org/10.1017/S0022112006009165 Published online by Cambridge University Press

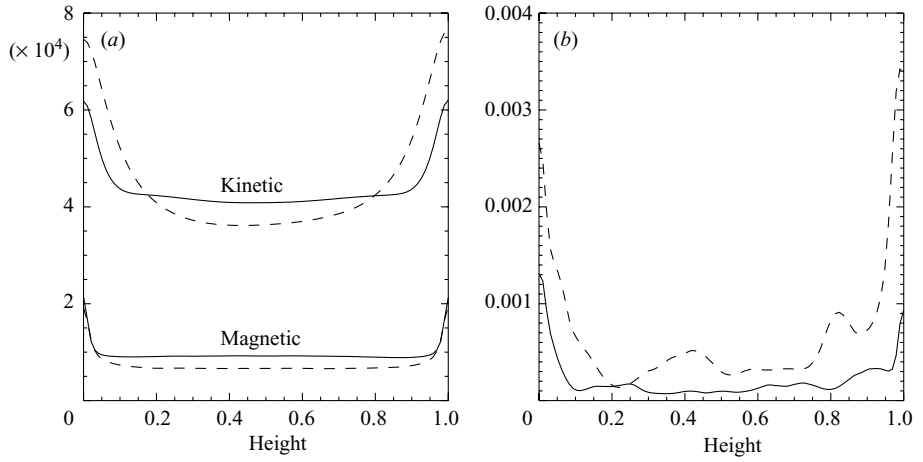


FIGURE 5. (*a*) Horizontally and time-averaged kinetic and magnetic energy densities for the rotating case (solid line) with $Ta = 5 \times 10^5$, $Ra = 10^6$, $\lambda = 10$, and non-rotating case (dashed line) with $Ta = 0$, $Ra = 5 \times 10^5$, $\lambda = 10$. (*b*) The z-dependence of Γ, the ratio of the energy in the mean field to the total magnetic energy, for the same two cases.

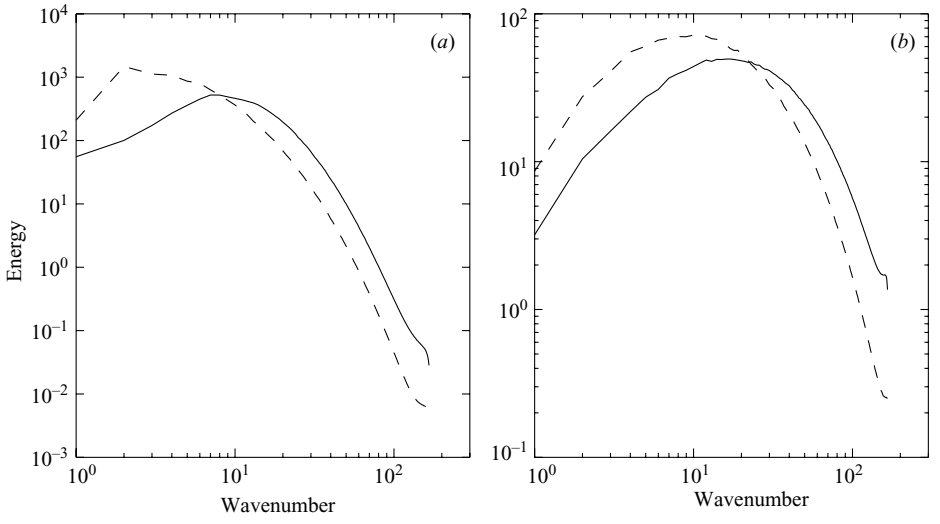


FIGURE 6. Horizontal power spectra for (*a*) velocity and (*b*) magnetic field. The solid and dashed lines correspond, respectively, to a rotating case with $Ta = 5 \times 10^5$, $Ra = 10^6$, and a non-rotating case with $Ta = 0$, $Ra = 5 \times 10^5$. In both cases $\lambda = 10$. The spectra were computed over the interior regions ($0.2 \leqslant z \leqslant 0.8$) of the simulations, and time-averaged over the time-stationary part of the solutions.

main difference between the two cases is a shift to higher wavenumbers of the curve corresponding to the rotating case, consistent with the overall reduction in size of the convective cells. An analogous quantity to $\Gamma(z)$ can be defined for the velocity. Its evaluation gives a value for both the non-rotating and rotating cases that is three orders of magnitude smaller than that for the magnetic field, thus confirming the complete absence of mean flows.

Finally, in figure 7 we plot the probability density functions (PDFs) of the horizontal components of the velocity and magnetic fields. We have considered two separate

https://doi.org/10.1017/S0022112006009165 Published online by Cambridge University Press

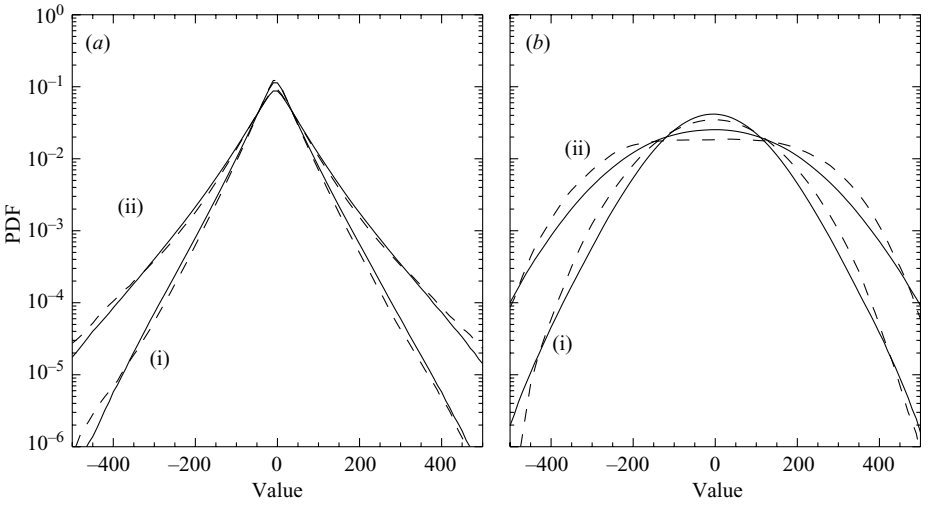


FIGURE 7. Probability distribution functions (PDFs) of fluctuations in (*a*) the horizontal magnetic field, and (*b*) horizontal velocity. Solid and dashed curves correspond to a rotating ($Ta = 5 \times 10^5$, $Ra = 10^6$, $\lambda = 10$) and a non-rotating ($Ta = 0$, $Ra = 5 \times 10^5$, $\lambda = 10$) case. The two sets of PDFs were computed, respectively, in (i) the interior regions ($0.2 \leqslant z \leqslant 0.8$), and in (ii) the boundary regions (all the rest).

ensembles, respectively consisting of the interior $0.2 \leqslant z \leqslant 0.8$ (see figure 5*a*) and the boundary regions (the rest). As has been noted several times in studies of convectively driven dynamos (Cattaneo 1999; Thelen & Cattaneo 2000), the velocity PDF is Gaussian while the PDF for the magnetic field is close to an exponential. What is remarkable is that the corresponding PDFs for the two cases are practically identical, indicating a very robust common mechanism for dynamo generation.

The preceding considerations compel us to address the issue of the lack of mean field in the rotating case. Why is the α-effect so spectacularly unsuccessful given that the system is demonstrably helical? Two possibilities readily come to mind. One is that the system has a turbulent α-effect (i.e. independent of η) that becomes strongly nonlinearly saturated (Kulsrud & Anderson 1992; Vainshtein & Cattaneo 1992; Gruzinov & Diamond 1994); the other is that the α-effect is slow (i.e. α decreases with decreasing η), and therefore tiny for large Rm, even kinematically. Either possibility is consistent with the results since $\Gamma \approx |\langle \boldsymbol{B} \rangle|^2 / u_{rms}^2 \approx Rm^{-1}$ (see figure 5*b*). These issues are addressed in the next section.

5. Calculation of the α-effect

An unambiguous way of calculating the α-effect is to impose a uniform mean field $\langle \boldsymbol{B} \rangle = (B_0, 0, 0)$, say, and to measure the average emf

$$\mathscr{E}_i = \langle \boldsymbol{u} \times \boldsymbol{B} \rangle_i = \alpha_{ij} \langle B \rangle_j. \tag{5.1}$$

Because of the anti-symmetry of α about the mid-plane, the only sensible average is over the upper (or lower) half of the volume. In order to investigate the two possibilities described above, it is imperative to compute the α-effect in the kinematic regime, i.e. in the regime in which the emf is proportional to the imposed mean field. For large Rm, this requires that the mean field be very weak. If we assume that the standard estimates for the nonlinear saturation of the α-effect apply (Vainshtein &

https://doi.org/10.1017/S0022112006009165 Published online by Cambridge University Press

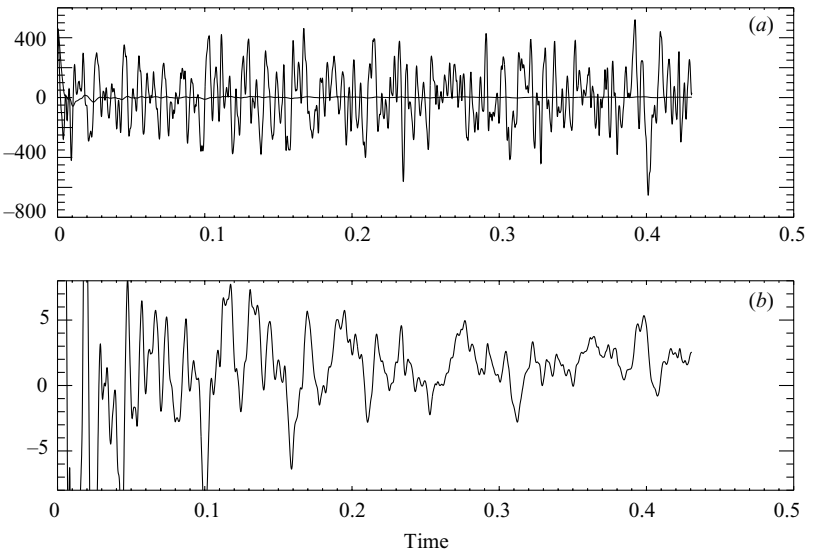


FIGURE 8. Time history of α_{11} for a case with $Ta = 5 \times 10^5$, $Ra = 10^6$, $\lambda = 5$ and $B_0 = 10$. The thick line in (a) corresponds to the time average up to time t of the signal, $\overline{\alpha}$. The same curve is plotted again in (b) with a more appropriate vertical axis.

Cattaneo 1992; Gruzinov & Diamond 1994), then in order to be in the kinematic regime, the mean field must satisfy $B_0 \lesssim Rm^{-1/2} u_{rms} \approx 6.3$ for the case above. Figure 8 shows the results of such a calculation with $\lambda = 5$ and $B_0 = 10$, where in figure 8(a) we plot $\alpha_{11} = \mathscr{E}_x / B_0$ as a function of time. It is immediately obvious that despite this being an average over many convective cells it is a strongly fluctuating quantity – even its sign appears to be ill defined. We attempt to improve the statistics by introducing the cumulative time average defined by

$$\overline{\alpha}(T) = \frac{1}{T} \int_0^T \alpha_{11}(t)\, \mathrm{d}t. \tag{5.2}$$

This is plotted in figure 8(a) as a thicker line. Superficially, on the scale of this figure, $\overline{\alpha}$ appears to be well behaved. However, closer inspection (figure 8b) shows that convergence to any well-defined value is painfully slow. Even after an averaging over 80 turnover times, its value is comparable with the error bars. Nevertheless, it can be concluded that its value, whatever it is, is comparable with u_{rms}/Rm. Thus, the α-effect in this case is either slow or, more improbably, is turbulent but with an extremely small coefficient. We can investigate this second possibility further by examining the variations of $\overline{\alpha}$ with B_0. The results of this analysis for a case with $\lambda = 5$ and $Ra = 5 \times 10^5$ are summarized in figure 9, where we show the cumulative averages for three values of B_0. The first case (figure 9a) has $u_{rms} = 140 \Rightarrow Rm = 700$; thus the conservative estimate for the mean field strength at the end of the kinematic phase is given by $140/\sqrt{700} \approx 5.3$. For this case $B_0 = 1$, which is well within the kinematic regime; nonetheless the statistics are so badly behaved that it is impossible even to determine the sign of the cumulative average. The situation improves with increasing mean field strength. For $B_0 = 10$, the value of $\overline{\alpha}$ is still fluctuating, but, at least, it is definitely positive. For $B_0 = 100$, it approaches a well-defined value. Regardless of the difficulties in determining the precise values of $\overline{\alpha}$, we can rule out the possibility that the α-effect is turbulent and that it becomes nonlinearly saturated. This would

https://doi.org/10.1017/S0022112006009165 Published online by Cambridge University Press

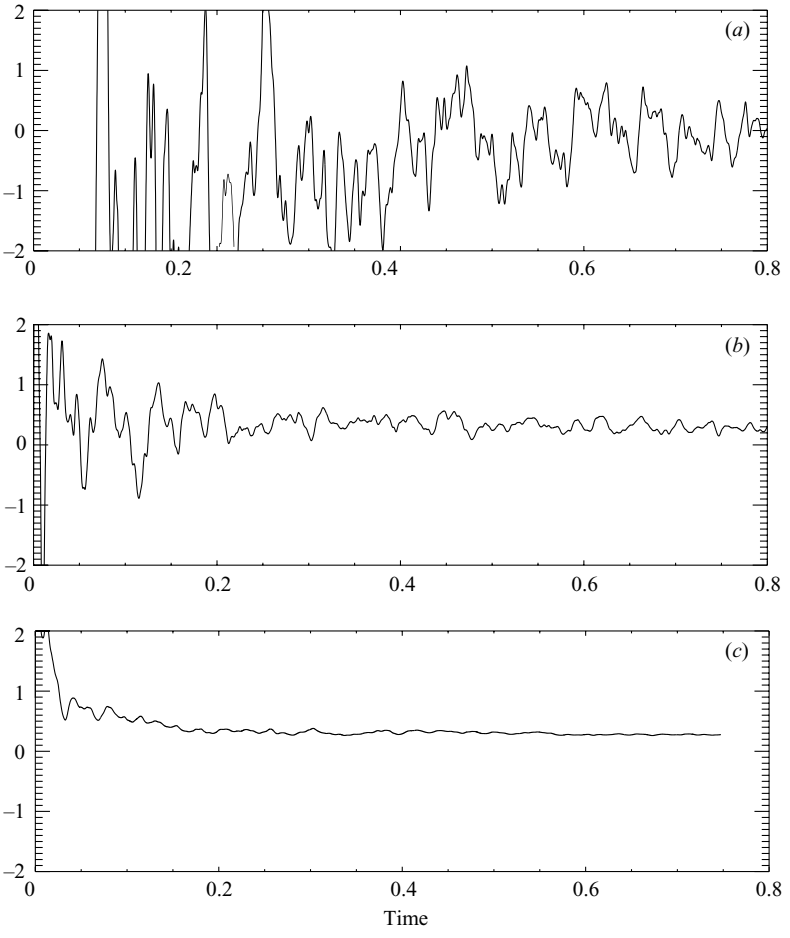


FIGURE 9. Time histories of the cumulative time average $\overline{\alpha}$ for three cases with $Ta = 5 \times 10^5$, $Ra = 5 \times 10^5$, $\lambda = 5$, and (*a*) $B_0 = 1$, (*b*) 10, (*c*) 100.

require a decrease in the value of α by a factor of 600 over the range of values considered, in clear contradiction to the results in figure 9. In fact, as far as we can see, $\overline{\alpha}$ remains roughly constant. Thus, the usual results concerning the so-called catastrophic α-quenching are irrelevant in this case.

Many of the difficulties that beset us in trying to obtain well-defined averages arise from the presence of large fluctuations in $\boldsymbol{B}$, and therefore in $\boldsymbol{u} \times \boldsymbol{B}$. It appears that an inevitable consequence of turbulent flows with large Rm is that they act as vigorous small-scale dynamos. Such systems are characterized by strong magnetic fluctuations that are completely unrelated to the magnitude of the mean field. We would therefore expect matters to be easier if small-scale dynamo action could be avoided. In this case, the magnetic fluctuations could be more easily controlled since they arise solely from interactions between the flow and the mean field. Indeed, for the present system there is a range of Ra ($59\,008 \leqslant Ra \lesssim 170\,000$) in which the fluid is convectively unstable, yet the motions do not support dynamo action. Towards the top of this range, the convection is already quite vigorous (see figure 1) and therefore we would expect some correspondence between the behaviour of α in this regime and in those with higher values of Ra.

https://doi.org/10.1017/S0022112006009165 Published online by Cambridge University Press

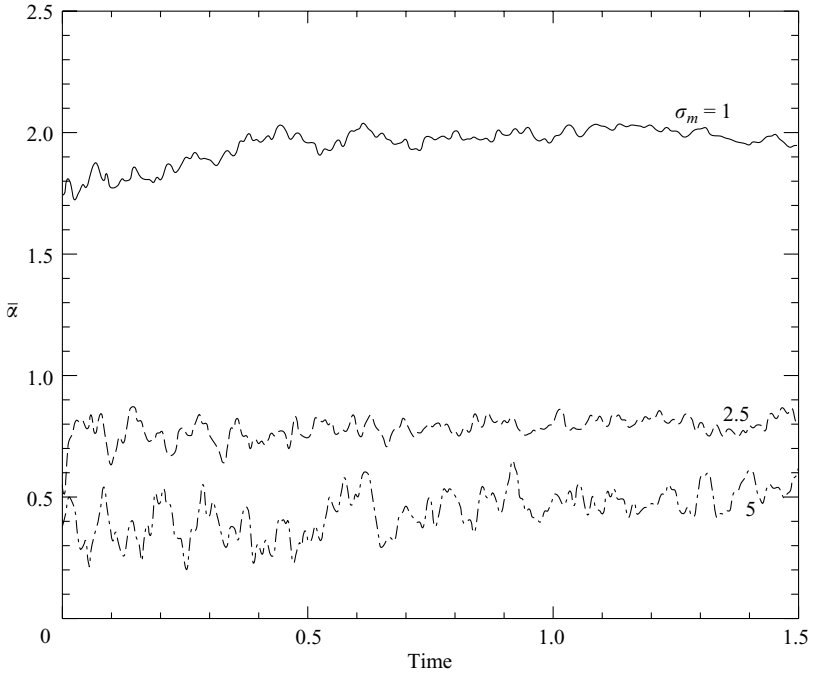


FIGURE 10. Time histories of the cumulative time average $\overline{\alpha}$ for three cases with $Ta = 5 \times 10^5$, $Ra = 1.5 \times 10^5$, $\lambda = 5$, $B_0 = 1$ and $\sigma_m = 5$, 2.5, 1.

Following these considerations we have carried out a series of simulations with $\lambda = 5$, $Ra = 150\,000$, and $\sigma_m = 5$, 2.5, 1. The calculation of α is summarized in figure 10, where we show the cumulative averages for the three cases. There are two points worthy of note. The first is that even in this regime the statistics leave something to be desired. It is thus becoming apparent that the problem really lies with the high value of Rm rather than with small-scale dynamo action *per se*. If Rm is large, the ratio between fluctuations and mean will be large, irrespective of self-excitation. The second is that $\overline{\alpha}$ *increases* with η, rather than being independent of it, thereby confirming our suspicion that the α-effect in this system is slow. Of course we know from considerations of first-order smoothing that for sufficiently small values of Rm this trend must reverse and α must eventually become linear in Rm.

We should note that the observed dependence of α on η indeed follows from the lack of large-scale dynamo action for this particular system. The horizontally averaged induction equation can be written as

$$\frac{\partial}{\partial t}\langle \boldsymbol{B} \rangle = \boldsymbol{e}_z \times \frac{\partial}{\partial z}\boldsymbol{\mathscr{E}} + \eta \frac{\partial^2}{\partial z^2}\langle \boldsymbol{B} \rangle. \tag{5.3}$$

The important point to notice is that the diffusion coefficient in (5.3) is η and not $\eta + \beta$, with β the eddy diffusivity (Childress & Soward 1972). This follows from the anisotropic nature of the averages arising from the existence of a separation of scales in the horizontal but not in the vertical. It follows immediately therefore that in the absence of dynamo action any α-effect cannot exceed a number of order η. Detailed calculations are, however, still necessary to compute the actual values.

https://doi.org/10.1017/S0022112006009165 Published online by Cambridge University Press

6. Discussion

Our simulations have shown that, as expected from consideration of the non-rotating case, vigorous rotating convection at high magnetic Reynolds number acts as a very efficient small-scale dynamo. The dynamo growth time is comparable with the turnover time, and the saturation amplitude of the magnetic fluctuations is comparable with the equipartition value. More unexpected was the complete failure of the system to act as a large-scale dynamo despite the helical nature of the turbulence. Indeed, we found levels of the mean field amplitude that were indistinguishable from those with no rotation. If this result is to be understood in terms of mean field theory, then the only conclusion to be drawn is that α is extremely small, controlled by the magnetic diffusion, even in the kinematic regime. Exactly why the dynamo growth rate is fast (independent of η) while the α-effect is slow (i.e. η-dependent) is an intriguing question. Clearly the problem is related to the nature of the sample space over which the average defining the α-effect is taken. At large values of Rm, the fluctuations in $\boldsymbol{u} \times \boldsymbol{b}$ have either sign and have huge magnitudes compared with the average value. This is in stark contrast to other statistical quantities, such as the helicity, for which the fluctuations are representative of the mean. It is interesting that, at least heuristically, we can interpret the fluctuating nature of $\boldsymbol{u} \times \boldsymbol{b}$ in terms of the original picture of Parker (1955) of cyclonic events and the current associated with twisted field loops. Even if the twisting motions always have the same handedness then, if the loops do not readily reconnect, we expect the fluctuations in the emf to change sign. The puzzle now is why is reconnection so ineffective? We have no definitive answer at this time, but clearly this issue is central to our understanding of magnetic field generation in terms of average quantities.

It is instructive to relate our results to those of earlier studies of dynamo action driven by rotating plane-layer convection. The problem was first investigated in depth by Childress & Soward (1972), and considerably extended into the weakly nonlinear regime by Soward (1974). In order to make analytic progress, these authors considered the case of strong rotation, slightly supercritical convection, and small magnetic Reynolds number. Strong rotation forces the cells to be extremely thin, allowing a strict ordering between horizontal and vertical derivatives; weak supercriticality results in the convection having simple planforms; small Rm justifies the use of the first-order smoothing approximation. It was shown by Soward (1974) that for certain planforms, dynamo action was possible. By construction, the resulting solutions have small fluctuations in the magnetic field relative to the mean; furthermore, the nonlinear state is characterized by a small ratio of magnetic to kinetic energy density. It is interesting to imagine how Soward's solutions may change as Rm is increased. There are two ways in which this can be achieved. One is by decreasing η while remaining close to marginal stability; in this approach, the structure of the velocity remains the same, at least kinematically, but the analysis has to be modified to account for the breakdown of the first-order smoothing approximation. The other is to keep η fixed, but to increase Ra so as to increase the amplitude of the convection – this is the path that links Soward's regime to ours; however, we should note that there must be an intervening regime in which the Soward dynamo has switched off and in which the dynamo that we find has not yet become operative. Thus, there is no simple relation between Soward's solutions and ours.

There has been a number of numerical studies of dynamo action in a rotating convective plane layer; of particular relevance to our investigation are the works of St Pierre (1993), Jones & Roberts (2000), Rotvig & Jones (2002) and Stellmach & Hansen (2004). Interestingly all of these authors found dynamo solutions in which

https://doi.org/10.1017/S0022112006009165 Published online by Cambridge University Press

the energy in the mean field is comparable with that in the fluctuations. It behoves us therefore to examine the causes of the striking differences between the character of their solutions and ours. St Pierre (1993) concentrated on dynamo solutions belonging to the so-called 'strong field branch'. It is well known that magnetic fields can facilitate instability in convective systems with strong rotation; this was demonstrated for magnetoconvection by Eltayeb & Roberts (1970) and for dynamos by Fautrelle & Childress (1982). St Pierre (1993) investigated a system with large Ta and subcritical Rayleigh number, and found nonlinear dynamo action with magnetic energy well in excess of the kinetic energy. These solutions require initial conditions of strong magnetization, and are therefore fundamentally different to those that have a well-defined kinematic regime. It is interesting to speculate whether, in our extended system and for substantially supercritical Rayleigh numbers, dynamo solutions belonging to the 'weak field branch' ever generate fluctuations large enough to cause a jump to the strong field branch. We, however, have never seen this behaviour despite long time integrations.

As in our study, the other three cases considered the growth of magnetic field from an initial state of weak magnetization. The biggest difference between these studies and ours is in the level of disorder of the underlying velocity field. Whereas our basic convection is characterized by a disordered cellular pattern, in all the other cases the structure of convection is more organized. We believe that it is this difference in planform appearance – disordered in one case, ordered in the others – that causes the average of the emf to be ill-behaved and tiny in the one case, and well-behaved and sizeable in the others. There are several factors that influence the organization of the convective pattern; for instance, the boundary conditions, the value of the Prandtl number, the horizontal size of the domain (the aspect ratio), and the strength of the thermal driving relative to the constraining influence of rotation (measured by, say, the inverse Rossby number). Of these differences, we think that the choice of boundary conditions is the least important. More important is the choice of Prandtl number, finite as opposed to infinite (Jones & Roberts 2000; Rotvig & Jones 2002), since it is known that infinite Prandtl number convection is more spatially organized (see, for example, Schmalzl, Breuer & Hansen 2002). Possibly most important are the horizontal size of the integration domain and the Rossby number. In a sufficiently small domain, regardless of the strength of the convective driving, only a few regular patterns are available to the system; whereas we have considered domains with aspect ratio of five or larger, the other studies have considered aspect ratios of one or smaller. At small Rossby numbers, rotation is overwhelmingly important and leads to a fairly well-ordered pattern of narrow convective cells; at $O(1)$ Rossby numbers, on the other hand, although rotation is still influential (hence the presence of helicity) it is no longer overly constraining. In most of our simulations, the Rossby number is $O(1/4)$; other simulations (e.g. Stellmach & Hansen 2004) have concentrated on the rotationally dominated regime and considered Rossby numbers of $O(10^{-3})$.

We should finish by addressing the problem of the generation of sizeable large-scale magnetic fields in astrophysical situations. There are two distinct questions. One is to identify the important physical processes, the other is to determine the formalism that should be used to describe them. Certainly, large-scale flows will be of importance (e.g. Ponty, Gilbert & Soward 2001) as may be the role of boundary conditions (e.g. Blackman & Field 2000). Indeed, we can think of many other 'non-universal' processes that may play a role in any specific circumstance. The thrust of this paper, however, concerns the applicability of mean field ideas to the description of field generation in astrophysical systems. The present study, and its comparison with the work of others,

https://doi.org/10.1017/S0022112006009165 Published online by Cambridge University Press

indicates that at high Rm and in extended systems, the α-effect is almost entirely determined by the nature of the statistical ensemble. An unambiguous determination of α requires time integration over an unpractically long interval, greatly exceeding all relevant dynamical time scales. Integration over reasonable – but still long – time scales reveals an average that is strongly fluctuating. This leads us to question the role of the α-effect in our understanding of mean field dynamo action at high Rm. As mentioned earlier, if α can be computed *a priori* from the velocity field then it has predictive power; if it can be determined from the solution in a reasonable way then it has interpretative power. If it cannot even be determined from the solution, then we may have to reconsider the relevance of some of these mean field ideas.

We would like to thank Professors C. A. Jones, M. R. E. Proctor, A. M. Soward and N. O. Weiss for useful discussions and helpful comments. The authors were supported in part by the NASA SR&T program at the University of Chicago. F.C. was also partially supported by a PPARC visiting fellowship.

REFERENCES

Blackman, E. G. & Field, G. B. 2000 Constraints on the magnitude of α in dynamo theory. *Astrophys. J.* **534**, 984–988.

Braginskii, S. I. 1964 Self excitation of a magnetic field during the motion of a highly conducting fluid. *Sov. Phys. JETP* **20**, 726–735.

Cattaneo, F. 1999 On the origin of magnetic fields in the quiet photosphere. *Astrophys. J.* **515**, L39–L42.

Cattaneo, F., Emonet. T. & Weiss, N. O. 2003 On the interaction between convection and magnetic fields. *Astrophys. J.* **588**, 1183–1198.

Cattaneo, F. & Hughes, D. W. 1996 Nonlinear saturation of the turbulent α-effect. *Phys. Rev.* E **54**, R4532–R4535.

Chandrasekhar, S. 1961 *Hydrodynamic and Hydromagnetic Stability*. Clarendon.

Childress, S. & Soward, A. M. 1972 Convection driven hydromagnetic dynamo. *Phys. Rev. Lett.* **29**, 837–839.

Eltayeb, I. A. & Roberts, P. H. 1970 On the hydromagnetics of rotating fluids. *Astrophys. J.* **162**, 699–701.

Fautrelle, Y. & Childress, S. 1982 Convective dynamos with intermediate and strong fields. *Geophys. Astrophys. Fluid Dyn.* **22**, 235–279.

Field, G. B., Blackman, E. G. & Chou, H. S. 1999 Nonlinear α-effect in dynamo theory. *Astrophys. J.* **513**, 638–651.

Gruzinov, A. V. & Diamond, P. H. 1994 Self-consistent theory of mean field electrodynamics. *Phys. Rev. Lett.* **72**, 1651–1654.

Jepps, S. A. 1975 Numerical models of hydromagnetic dynamos. *J. Fluid Mech.* **67**, 625–645.

Jones, C. A. & Roberts, P. H. 2000 Convection-driven dynamos in a rotating plane layer. *J. Fluid Mech.* **404**, 311–343.

Krause, F. & Rädler, K.-H. 1980 *Mean-Field Magnetohydrodynamics and Dynamo Theory*. Pergamon.

Kulsrud, R. M. & Anderson, S. W. 1992 The spectrum of random magnetic fields in the mean field dynamo theory of the Galactic magnetic field. *Astrophys. J.* **396**, 606–630.

Meneguzzi, M. & Pouquet, A. 1989 Turbulent dynamos driven by convection. *J. Fluid Mech.* **205**, 297–318.

Moffatt, H. K. 1978 *Magnetic Field Generation in Electrically Conducting Fluids*. Cambridge University Press.

Parker, E. N. 1955 Hydromagnetic dynamo models. *Astrophys. J.* **122**, 293–314.

Ponty, Y., Gilbert, A. D. & Soward, A. M. 2001 Kinematic dynamo action in large magnetic Reynolds number flows driven by shear and convection. *J. Fluid Mech.* **435**, 261–287.

https://doi.org/10.1017/S0022112006009165 Published online by Cambridge University Press

Pouquet, A., Frisch, U. & Léorat, J. 1976 Strong MHD helical turbulence and the nonlinear dynamo effect. *J. Fluid Mech.* **77**, 321–354.

Rotvig, J. & Jones, C. A. 2002 Rotating convection-driven dynamos at low Ekman number. *Phys. Rev.* E **66**, 056308:1–15.

Rüdiger, G. 1989 *Differential Rotation and Stellar Convection: Sun and Solar-Type Stars*. Gordon and Breach.

St Pierre, M. G. 1993 The strong field branch of the Childress–Soward dynamo. In *Theory of Solar and Planetary Dynamos* (ed. M. R. E. Proctor, P. C. Matthews & A. M. Rucklidge). pp. 295–302. Cambridge University Press.

Schmalzl, J., Breuer, M. & Hansen, U. 2002 The influence of the Prandtl number on the style of vigorous thermal convection. *Geophys. Astrophys. Fluid Dyn.* **96**, 381–403.

Soward, A. M. 1974 A convection driven dynamo I. The weak field case. *Phil. Trans. R. Soc. Lond.* A **275**, 611–651.

Steenbeck, M., Krause, F. & Rädler, K.-H. 1966 A calculation of the mean electromotive force in an electrically conducting fluid in turbulent motion, under the influence of Coriolis forces. *Z. Naturforsch.* **21a**, 369–376.

Stellmach, S. & Hansen, U. 2004 Cartesian convection driven dynamos at low Ekman number. *Phys. Rev.* E **70**, 056312:1–16.

Thelen, J.-C. & Cattaneo, F. 2000 Dynamo action driven by convection: the influence of magnetic boundary conditions. *Mon. Not. R. Astr. Soc.* **315**, L13–L17.

Vainshtein, S. I. & Cattaneo, F. 1992 Nonlinear restrictions on dynamo action. *Astrophys. J.* **393**, 165–171.

Yoshimura, H. 1975 A model of the solar cycle driven by the dynamo action of the global convection in the solar convection zone. *Astrophys. J. Suppl.* **29**, 467–494.

https://doi.org/10.1017/S0022112006009165 Published online by Cambridge University Press